

On semiconductor–metal transition in FeSi induced by ultrahigh magnetic field

Yu. B. Kudasov*, D. A. Maslov

Sarov Physics and Technology Institute, NRNU "MEPhI", 6 Dukhov st., Sarov, 607186, Russia

Russian Federal Nuclear Center - VNIIEF, 37 Mira av., Sarov, 607188, Russia

Abstract

At low temperatures, iron monosilicide is a strongly correlated narrow-gap semiconductor. A first order transition to metal state induced by magnetic field was observed for the first time at 355 T in Ref. [Yu. B. Kudasov *et al.*, JETP Lett. **68** (1998) 350]. However, recently a smooth transition from 230 T to 270 T was found under similar conditions in Ref. [D. Nakamura *et al.*, Phys. Rev. Lett. **127** (2021) 156601]. This discrepancy goes far beyond experimental errors and deserves a careful study. A methodological analysis of inductive and RF techniques of conductivity measurements shows that the difference of these critical magnetic field estimations stems from a divergence in dynamic ranges of the techniques. In fact, the above mentioned methods supplement each other. The semiconductor-metal transition under magnetic field in FeSi is a complex phenomenon which occurs at the wide range of magnetic fields.

Keywords: high magnetic field, phase transition, FeSi, AC conductivity, magnetization, magnetic flux compression, Kondo insulator

1. Introduction

Iron monosilicide (FeSi) has been attracting attention of theorists and experimentalists for several decades [1, 2, 3, 4, 5]. It is a non-magnetic metal above room temperature[1, 5]. However, FeSi becomes a narrow-gap

*Corresponding author

Email address: kudasov@ntc.vniief.ru (Yu. B. Kudasov)

semiconductor below 100 K with the gap width of about 60 meV [2, 5]. Effective masses of mobile charge carriers on the top of the valence band and the bottom of the conduction band grow with decreasing temperature and reach extremely large values ($m \sim 100m_0$), which makes it possible to attribute FeSi to a rather exotic group of heavy fermion compounds without f-elements [2, 4]. Comparison of experimental data with results of calculations of the electronic structure demonstrated that the heavy carriers in FeSi appeared due to strong electronic correlations in bands formed mainly by iron d-orbitals [6, 7]. This problem was investigated in the framework of the Hubbard model [8]. The hypothesis of FeSi as a Kondo insulator was widely discussed [9, 10]. However, a realistic model should include strong multiorbital correlations [7].

Below 70 K another transport anomalies in FeSi are observed. They are ascribed to quasiparticles of spin-polaron type, which form a very narrow band about 6 meV wide inside the gap [11]. During the last decade, few Kondo insulators were proven to be a topological insulator including SmB₆, which thermodynamical and transport low-temperature properties were similar to those of FeSi [12, 13, 14]. The existence of a thin layer with high conductivity on the surface of iron monosilicide was recently experimentally demonstrated on ultra-thin single crystal samples [4, 15]. Moreover, the observed hysteresis of the Hall effect demonstrated that the 2D conductive surface layer in FeSi is ferromagnetic with a non-magnetic bulk state [15].

At low temperatures and moderate magnetic fields, anisotropic magnetoresistance was revealed in FeSi [4]. The anisotropy was a consequence of an interplay of the surface and bulk charge mobile carriers [12] and transport properties of FeSi was described by means of two-band model [3]. Under ultrahigh magnetic field (above 100 T), the gap in electron spectrum of FeSi should be suppressed by the Zeeman splitting of the conduction and valence bands edges. The LDA+U [16] and LSDA [17, 18] calculations gave an estimation of the critical magnetic field of the transition to the metallic state of about 170 T at $T = 0$ K. In fact, the mechanism of metallization involves a renormalization of the quasiparticle bands by spin fluctuations that could greatly shift this value [19].

For the first time, the semiconductor-metal transition induced by ultrahigh magnetic field in FeSi was experimentally observed and studied in Ref. [20, 21] using induction magnetization measurements and radio-frequency (RF) contactless conductivity measurements. At $T = 5$ K it was observed at 355 T and was accompanied by a step in the magnetic moment. At $T = 78$ K

there was a smooth increase in conductivity, and without the step in the magnetic moment. Qualitatively, this was in good agreement with the theoretical magnetic phase diagram [16]: a phase transition of the first kind from singlet semiconductor to ferromagnetic metal existed at low temperatures and a smooth transition did above a certain critical temperature. Recently, FeSi was studied under ultrahigh magnetic field at various temperatures using a similar RF measuring technique [22] and at $T = 6$ K an extended transition was observed, which ended at about 275 T. The discrepancy in the results of Ref. [20, 21, 22] goes far beyond experimental errors and deserves a careful study.

A magnetic flux compression technique is the only possibility to investigate transport and magnetic properties of substances at 300 T and above [23]. The fast flux compression is realized by means of high explosives (HEC) [24] or ponderomotive electromagnetic forces (EMC) [25]. The both approaches were used in the investigations of FeSi: the first one was implemented in MC-1 generator, which was used in Ref. [20, 21], the EMC technique was applied in Ref. [22]. A time dependence of magnetic field in these devices had a complex shape: a slow initial part up to approximately 16 T and fast growth of the magnetic field under the flux compression during about 15 μ s. The final part of the magnetic field pulse of the MC-1 generator is shown in Fig. 1. It is very similar to that of EMC facility. It should be mentioned that the ultrahigh magnetic field generation is accompanied by intensive electromagnetic noises, and, that is why, a choice of measuring methods is greatly limited [24].

In the present article, we consider methodological aspects of inductive and RF conductivity measuring techniques and discuss the discrepancy of the results on the semiconductor–metal transition under the ultrahigh magnetic field in FeSi.

2. Inductive conductivity measurement

The compensation inductive technique is widely used for magnetization and conductivity measurements in pulsed magnetic fields and, in particular, in ultrahigh magnetic fields [20, 26]. The compensation sensor is a pair of small identical coils with counter-winding, which axes are oriented along the external magnetic field (see Fig. 2). A measured sample is installed in one of the coils. In case of a long sample, the electromotive force generated by

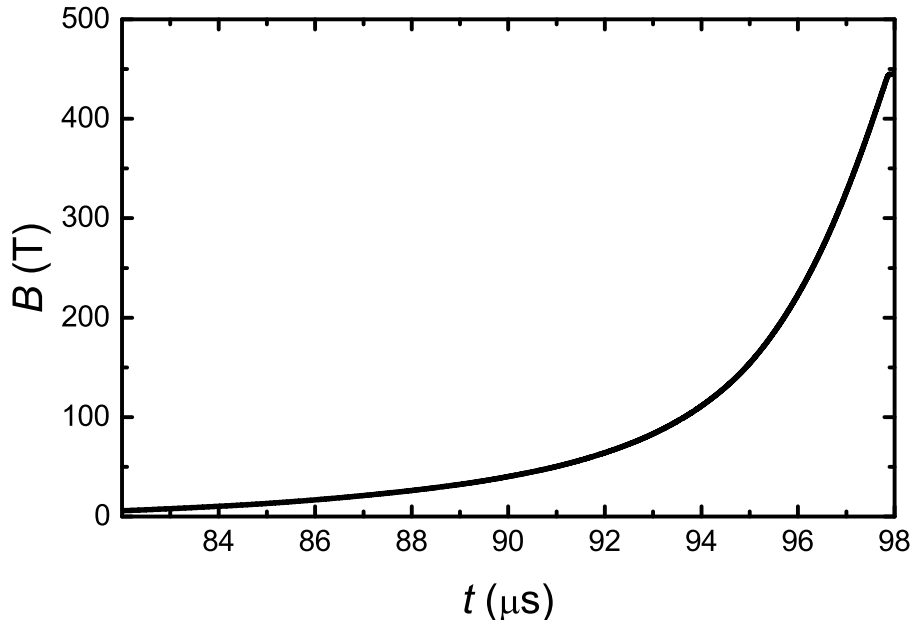


Figure 1: The final part of the magnetic field pulse of MC-1 generator.

the sensor consists of two components [27]:

$$\mathcal{E} = \alpha\mu_0\dot{H} + \mu_0NS\dot{M}, \quad (1)$$

where H and M are the magnetic intensity and magnetization (or specific magnetic moment appeared due to eddy currents), μ_0 is the permeability of free space, N is the number of turns, S is the sample sectional area, and α is the coefficient, which is proportional to compensation error. From Eq. (1) one can see that there is an additional background signal which is proportional to the time derivative of the magnetic flux density. It can be eliminated by comparing it with a background signal obtained from the pick-up coil which is used for magnetic field measurement. The procedure is illustrated in Fig. 3 where signals from Ref. [20] at $T = 77$ K are shown.

In a conductive sample, a pulsed magnetic field generates eddy currents, which induce the specific magnetic moment M . To separate the contribution of the sample conductivity to the signal from intrinsic magnetization, an additional measurement has to be performed with a powder sample in dielectric matrix [21]. It gives the magnetization response only.

Under ultrahigh magnetic fields a number of specific requirements to the sensor have to be taken into account. For example, due to high rates of

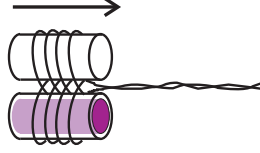


Figure 2: Schematic view of compensated inductive sensor. The arrow denotes the external magnetic field direction.

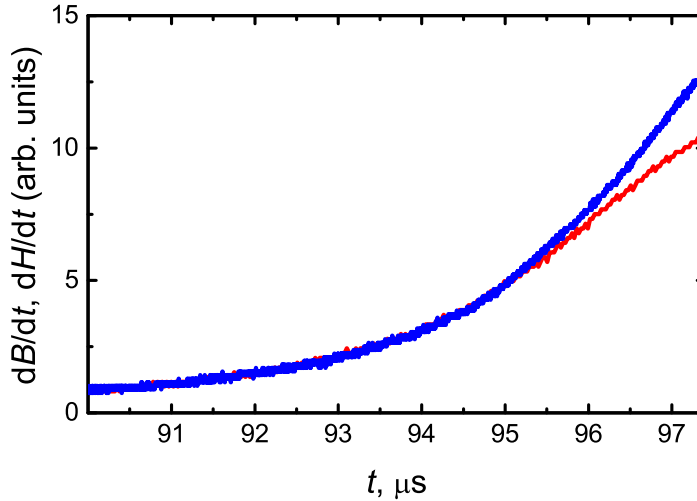


Figure 3: Normalized background signal from pick-up coil (blue line) and compensation sensor signal (red line) [20].

magnetic field growth a voltage reaches huge values even in miniature sensors and can cause an electrical breakdown. To eliminate the problem a special type of winding can be used [27].

When conductivity is small, that is, the magnetic field generated by eddy currents in the sample is much less than the external pulsed magnetic field, conductivity can be determined from the measured electromotive force by means of the following expression [21]

$$\sigma(t) = \frac{8}{\pi R^4 \mu_0 \dot{B} N} \int_0^t \mathcal{E}(\tau) d\tau \quad (2)$$

where R is the sample radius. Here the sample is assumed to be a long cylinder. The integral form of this equation partially suppresses an effect of noises.

Eq. (2) allows estimating a threshold of sensitivity. To do this, the integral in the right side of the equation should be replaced by its minimal detectable value. Then, the threshold of sensitivity is inversely proportional to the time derivative of the magnetic flux density, which varies drastically during the pulse of the magnetic field as one can see in Fig. 1. The upper bound of the dynamical range is defined by a non-linear regime of magnetic field diffusion into the sample while the conductivity becomes sufficiently high. In practice, however, it was limited to the maximum value of the recorded signal [21].

It should be mentioned that an effect of the finite length of the sample on the measurement results can be taken into account by means of a magnetostatic reciprocity theorem [26].

3. RF conductivity measurement

The RF method of conductivity measurement has been successfully applied in ultrahigh magnetic field for a long time [28, 20, 21, 29, 30, 22, 31]. The absence of contacts with a sample and using a narrow frequency band makes it possible to suppress electromagnetic interference that are induced by ultrahigh magnetic field. Initially, two small flat coils with a typical diameter of 3 to 5 mm were used, each of which contained several turns. The coils were positioned coaxially with each other. A test sample in the form of a plate was inserted into a small gap between the coils [28]. The axis of the coils was oriented perpendicular to the external magnetic field to reduce the induced voltage. An RF signal from the generator was fed to one of the coils, and the signal from the other coil was sent to the oscilloscope. An amplitude of the measured signal depended on the conductivity of the sample. An analysis of the electrodynamics of the measuring unit showed that there is a wide area of linear conductivity response.

Currently, a single-coil measuring unit is used [20, 29, 22, 31] (see Fig. 4). It combines the function of the transmitting and receiving coils. A probing RF signal is applied to the coil through a bandpass filter and cable line. A reflected signal is generated by eddy currents in the sample. It propagates through the same cable and bandpass filter. Then the reflected signal is separated from the probe one. The electrodynamics of RF measurements in the two-coil system was thoroughly investigated [28]. Below we will consider a single-coil system using the same approach.

The RF measuring unit has an axial symmetry (Fig. 4). The vector potential in cylindrical coordinates (r, z, φ) is determined by the following

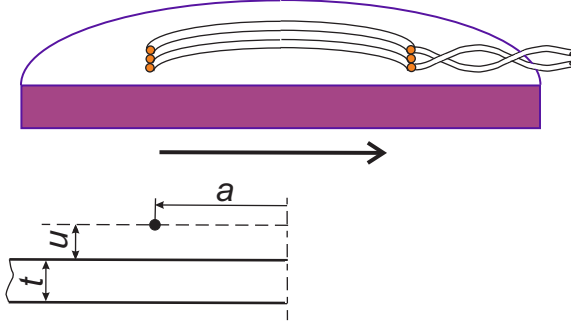


Figure 4: Schematic view of RF single-coil measuring unit (the coil and sample) and model representation (bottom panel). The arrow denotes the external magnetic field direction.

expression [28]

$$\frac{\partial^2 A}{\partial r^2} + \frac{1}{r} \frac{\partial A}{\partial r} - \frac{A}{r^2} + \frac{\partial^2 A}{\partial z^2} = i\omega\mu_0\sigma A, \quad (3)$$

where $A \equiv A_\varphi$ is the φ -component of the vector potential, ω is the circular frequency of the probe signal.

By separating the variables r and z the Eq. (3) is reduced to Bessel's equation of the first kind on r and the following equation on z

$$\frac{\partial^2 A}{\partial z^2} = k'^2 A, \quad (4)$$

where $k'^2 = k^2 + i\omega\mu_0\sigma$, and k is the separation parameter. Then, a solution of Eq. 3 under the physical boundary condition at the z -axis can be written as

$$A(r, z) = \int_0^\infty [a(k)e^{k'z} + b(k)e^{-k'z}] J_1(kr) dk, \quad (5)$$

where $a(k)$ and $b(k)$ are the coefficients, $J_1(kr)$ is the Bessel function of the first kind. The whole space is separated into four regions as shown in the bottom panel of Fig. 4. The coefficients $a(k)$ and $b(k)$ in each of them are determined by the boundary conditions [28]. There is a significant difference with the two-coil system. Namely, the total voltage on the coil is divergent as it is on the transmitting coil in the two-coil system. This is an effect of the approximation of infinitely thin coil. That is why, instead of an amplitude

of the total signal we obtain a normalized amplitude of the reflected signal induced by the eddy currents. It has the following complex form

$$R = \frac{U}{U_\infty} = 2 \int_0^\infty \frac{(k'^2 - k^2) \exp(-2ku) \sinh(k't) J_1^2(ka)}{(k + k')^2 \exp(k't) - (k' - k)^2 \exp(-k't)} dk \times \left[\int_0^\infty \exp(-2ku) J_1^2(ka) dk \right]^{-1}, \quad (6)$$

where a , t , and u are the coil radius, sample thickness, and width of the gap between the coil and sample Fig. 4, U_∞ is the amplitude of the reflected signal at $\sigma \rightarrow \infty$.

An amplitude and phase of the reflected signal are shown in Fig. 5. The geometrical parameters correspond to those of measuring unit in Ref.[21]. Since the amplitude and phase of the reflected signal depend on the product σf , the sensitivity threshold of conductivity inversely proportional to the frequency f . Under heavy electromagnetic interferences the dynamical range of the technique is usually no greater than two orders of magnitude of conductivity.

The analysis above gives a good description for the RF measurements at relatively low frequency band ($f \approx 50$ MHz) [28, 21, 29]. At the same time, while high frequency is applied ($f \approx 500 \div 700$ MHz) [22], a role of interturn and coil-sample capacitances increases. Therefore, the coil becomes a resonant circuit, and the analysis of the measuring unit operation becomes more complex although the underlying physical phenomenon remains the same. The operation of high-frequency measuring unit was studied in detail in Ref. [31].

4. Semiconductor-metal transition in FeSi

Experimental data from Ref. [21] and [22] are shown in Fig. 6 together with estimations of dynamical ranges corresponding to different techniques. One can see that they are in a reasonable agreement with each other. The RF technique at 700 MHz [22] was sensitive to much lower conductivity than that at 50 MHz and even more so the inductive compensation method. That is why, it gave the magnetic field dependence of conductivity starting from the initial values up to about 10^2 [Ohm cm] $^{-1}$ at 6 K and 10^3 [Ohm cm] $^{-1}$ at 53 K. The inductive technique had the much higher sensitivity threshold and

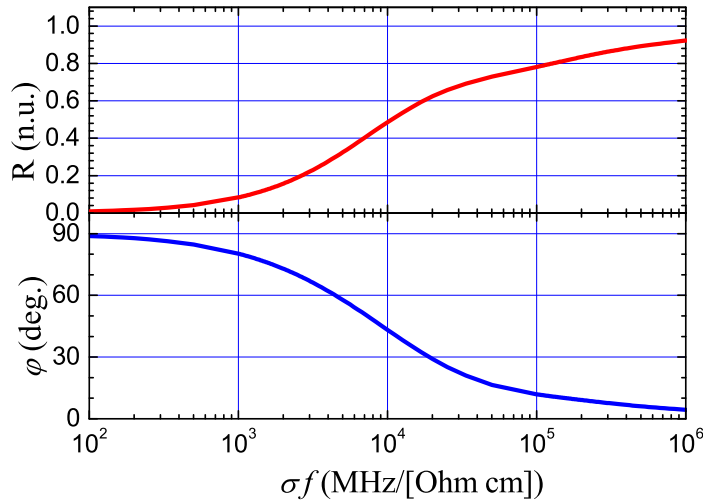


Figure 5: Amplitude R and phase φ of the normalized reflected signal of the RF single-coil measuring unit (Eq. 6) as a function of sample conductivity and frequency of the probe signal. Parameters correspond to Ref. [21]: $a = 1.5$ mm, $t = 0.3$ mm, $u = 0.2$ mm (see Fig. 4).

provided measurement above these values that occurred at higher magnetic field. One can see in Fig. 6 that the low-temperature field dependencies of conductivity of Ref. [21, 22] are in a reasonable agreement and supplement each other.

On the other hand, the results in Fig. 6 demonstrate that the semiconductor-metal transition in FeSi is a complex phenomenon which is extended in magnetic field [21, 22]. Magnetoresistance of FeSi in moderate magnetic field up to 10 T is determined by the interplay of the surface and bulk conductivity [4, 3, 12]. At higher magnetic field the in-gap spin-polaron-like states should play an important role because their characteristic energy scale is about 10 meV [11]. Then, the collapse of the intrinsic band gap occurs at ultrahigh magnetic fields. The first order transition with the magnetization step was observed at 5 K, and it was absent at 77 K [21]. The line of the first order transition with the critical point in the magnetic phase diagram [16] is still an open question which can be resolved by magnetization measurements at intermediate temperatures.

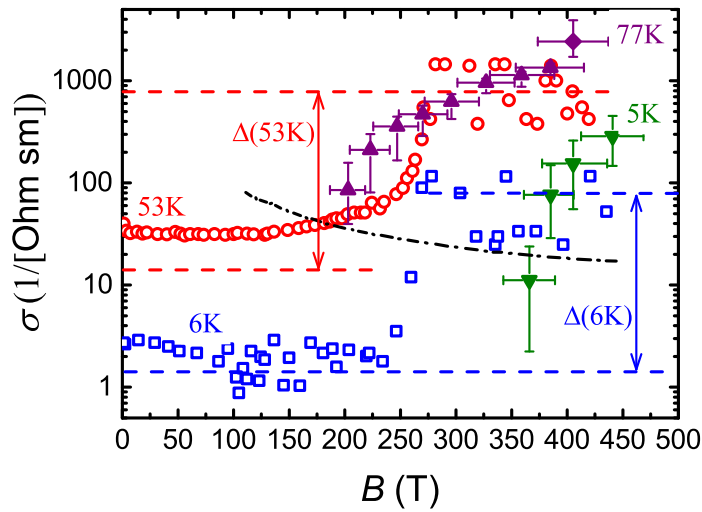


Figure 6: Magnetic field dependence of conductivity of FeSi at different initial temperatures. The full and open symbols correspond to the results of Ref. [21] and [22], correspondingly. The dash lines are estimations of the dynamical ranges $\Delta(T)$ [22, 31], the dash-dot black line is the low threshold of the inductive technique sensitivity (see Eq. 2). The circles and squares are RF measurements at 700 MHz [22], the diamond is that at 50 MHz [21], the up- and down-triangles demonstrate the results of inductive measurements [21]

5. Acknowledgement

The work was supported by National Center Physics and Mathematics (project "Investigation under high and ultrahigh magnetic fields"). The authors would like to thank Professor A.E. Dubinov for valuable comments.

References

References

- [1] V. Jaccarino, G. K. Wertheim, J. H. Wernick, L. R. Walker, S. Araj, Paramagnetic excited state of fesi, *Phys. Rev.* 160 (1967) 476. doi:10.1103/PhysRev.160.476.
- [2] Z. Schlesinger, Z. Fisk, H.-T. Zhang, M. B. Maple, J. F. DiTusa, G. Aeppli, Unconventional charge gap formation in fesi, *Phys. Rev. Lett.* 71 (1993) 1748. doi:10.1103/PhysRevLett.71.1748.
- [3] S. Paschen, E. Felder, M. A. Chernikov, L. Degiorgi, H. Schwer, H. R. Ott, D. P. Young, J. L. Sarrao, Z. Fisk, Low-temperature transport, thermodynamic, and optical properties of fesi, *Phys. Rev. B* 56 (1997) 12916. doi:10.1103/PhysRevB.56.12916.
- [4] Y. Fang, S. Ranc, W. Xied, S. Wange, Y. S. Menge, M. B. Maple, Evidence for a conducting surface ground state in high-quality single crystalline fesi, *PNAS* 115 (2018) 8558. doi:10.1073/pnas.1806910115.
- [5] S. Changdar, S. Aswartham, A. Bose, Y. Kushnirenko, G. Shipunov, N. C. Plumb, M. Shi, A. Narayan, B. Buchner, S. Thirupathaiyah, Electronic structure studies of fesi: A chiral topological system, *Phys. Rev. B* 101 (2020) 235105. doi:10.1103/PhysRevB.101.235105.
- [6] M. Arita, K. Shimada, Y. Takeda, M. Nakatake, H. Namatame, M. Taniguchi, H. Negishi, T. Oguchi, T. Saitoh, A. Fujimori, T. Kanomata, Angle-resolved photoemission study of the strongly correlated semiconductor fesi, *Phys. Rev. B* 77 (2008) 205117. doi:10.1103/PhysRevB.77.205117.
- [7] J. M. Tomczak, K. Haule, G. Kotliar, Thermopower of the correlated narrow gap semiconductor fesi and comparison to rusi, in: V. Zlatic,

- A. Hewson (Eds.), *New Materials for Thermoelectric Applications: Theory and Experiment*, Springer, Dordrecht, The Netherlands, 2013, p. 45. doi:10.1007/978-94-007-4984-94.
- [8] V. Glushkov, S. Demishev, M. Kondrin, A. Pronin, I. Voskoboinikov, N. Sluchanko, V. Moshchalkov, A. Menovsky, The regime of hubbard correlations in fesi, *Physica B* 312-313 (2002) 509. doi:10.1016/S0921-4526(01)01329-1.
- [9] Z. Schlesinger, Z. Fisk, H.-T. Zhang, M. Maple, Is fesi a kondo insulator?, *Physica B* 237-238 (1997) 460. doi:10.1016/S0921-4526(97)00137-3.
- [10] M. Klein, D. Zur, D. Menzel, J. Schoenes, K. Doll, J. Roder, F. Reinert, Evidence for itineracy in the anticipated kondo insulator fesi: A quantitative determination of the band renormalization, *Phys. Rev. Lett.* 101 (2008) 046406. doi:10.1103/PhysRevLett.101.046406.
- [11] V. V. Glushkov, I. B. Voskoboinikov, S. V. Demishev, I. V. Krivitskii, A. Menovsky, V. V. Moshchalkov, N. A. Samarin, N. E. Sluchanko, Spin-polaron transport and magnetic phase diagram of iron monosilicide, *JETP* 99 (2004) 394. doi:10.1134/1.1800197.
- [12] A. Breindel, High magnetic field investigations of correlated electron quantum materials, Phd dissertation, University of California, San Diego, USA (2021).
- [13] A. Breindel, Y. Deng, C. M. Moir, Y. Fang, S. Ran, H. Lou, S. Li, Q. Zeng, L. Shu, C. T. Wolowiec, I. K. Schuller, P. F. S. Rosa, Z. Fisk, J. Singleton, M. B. Maple, Probing fesi, a d-electron topological kondo insulator candidate, with magnetic field, pressure, and microwavesarXiv:Arxiv:Cond-mat2203.12839.
- [14] J. Kim, C. Jang, X. Wang, J. Paglione, S. Hong, J. Lee, H. Choi, D. Kim, Electrical detection of the surface spin polarization of the candidate topological kondo insulator smb₆, *Phys. Rev. B* 99 (2019) 245148. doi:10.1103/PhysRevB.99.245148.
- [15] Y. Ohtsuka, N. Kanazawa, M. Hirayama, A. Matsui, T. Nomoto, R. Arita, T. Nakajima, T. Hanashima, V. Ukleev, H. Aoki, M. Mogi,

- K. Fujiwara, A. Tsukazaki, M. Ichikawa, M. Kawasaki, Y. Tokura, Emergence of spin-orbit coupled ferromagnetic surface state derived from zak phase in a nonmagnetic insulator fesi, *Sci. Adv.* 7 (2021) eabj0498. doi:10.1126/sciadv.abj0498.
- [16] V. I. Anisimov, S. Y. Ezhov, I. S. Elfimov, I. V. Solovyev, T. M. Rice, Singlet semiconductor to ferromagnetic metal transition in fesi, *Phys. Rev. Lett.* 76 (1996) 1735. doi:10.1103/PhysRevLett.76.1735.
- [17] E. Kulatov, H. Ohta, T. Arioka, S. Halilov, L. Vinokurova, First-order metamagnetic transition in iron monosilicide, *J. Phys.: Cond. Matt.* 9 (1997) 9043. doi:10.1088/0953-8984/9/42/018.
- [18] T. Arioka, E. Kulatov, H. Ohta, S. Halilov, L. Vinokurova, First-principle band calculation of fesi under megagauss field, *Physica B* 246—247 (1998) 541. doi:10.1016/S0921-4526(97)00981-2.
- [19] A. A. Povzner, A. G. Volkov, P. V. Bayankin, Spin fluctuations and electronic semiconductor-metal transitions in iron monosilicide, *Phys. Solid State* 40 (1998) 1305. doi:10.1134/1.1130550.
- [20] Y. B. Kudasov, A. I. Bykov, M. I. Dolotenko, N. P. Kolokol'chikov, M. P. Monakhov, I. M. Markevtsev, V. V. Platonov, V. D. Selemir, O. M. Tatsenko, A. V. Filippov, A. G. Volkov, A. A. Povzner, P. V. Bayankin, V. G. Guk, V. V. Kryuk, Semiconductor-metal transition in fesi in ultrahigh magnetic fields up to 450 t, *JETP Letters* 68 (1998) 350. doi:10.1134/1.567872.
- [21] Y. B. Kudasov, A. I. Bykov, M. I. Dolotenko, N. P. Kolokol'chikov, M. P. Monakhov, I. M. Markevtsev, V. V. Platonov, V. D. Selemir, O. M. Tatsenko, A. V. Filippov, A. G. Volkov, A. A. Povzner, P. V. Bayankin, V. G. Guk, V. V. Kryuk, Semiconductor-metal transition in fesi in an ultrahigh magnetic field, *JETP* 89 (1999) 960. doi:10.1134/1.558938.
- [22] D. Nakamura, Y. H. Matsuda, A. Ikeda, A. Miyake, M. Tokunaga, S. Takeyama, Magnetoconduction in the correlated semiconductor fesi in ultrastrong magnetic fields up to a semiconductor-to-metal transition, *Phys. Rev.Lett.* 127 (2021) 156601. doi:10.1103/PhysRevLett.127.156601.

- [23] G. Shneerson, M. Dolotenko, S. Krivosheev, Strong and Superstrong Pulsed Magnetic Fields Generation, de Gruyter Studies in Mathematical Physics, Walter de Gruyter, 2014. doi:10.1515/9783110252576.
- [24] G. V. Boriskov, A. I. Bykov, M. I. Dolotenko, N. I. Egorov, Y. B. Kudasov, V. V. Platonov, V. D. Selemir, O. M. Tatsenko, Research in ultrahigh magnetic field physics, Phys. Usp. 54 (2011) 421. doi:10.3367/UFNe.0181.201104n.0441.
- [25] D. Nakamura, A. Ikeda, H. Sawabe, Y. H. Matsuda, S. Takeyama, Record indoor magnetic field of 1200 t generated by electromagnetic flux-compression, Rev. Sci. Instr. 89 (2018) 095106. doi:10.1063/1.5044557.
- [26] A. Kirste, Magnetization measurements in ultrahigh magnetic fields, Phd dissertation, Humboldt University, Berlin, Germany (2004).
- [27] Y. B. Kudasov, Megagauss magnetization measurements, Physica B 294-295 (2001) 684. doi:10.1016/S0921-4526(00)00744-4.
- [28] T. Sakakibara, T. Goto, N. Miura, Contactless transport measurements of metals in pulsed magnetic fields, Rev. Sci. Instr. 60 (1989) 444. doi:10.1063/1.1140398.
- [29] Y. B. Kudasov, High-frequency conductivity measurements by a contactless method in superhigh magnetic fields, Instr. Exp. Tech. 42 (1999) 527.
- [30] Y. B. Kudasov, A. V. Filippov, Measurements of high-frequency complex impedances in fast processes, Instr. Exp. Tech. 50 (2007) 806. doi:10.1134/S0020441207060140.
- [31] D. Nakamura, M. M. Altarawneh, S. Takeyama, Radio frequency self-resonant coil for contactless ac-conductivity in 100 t class ultra-strong pulse magnetic fields, Meas. Sci. Technol. 29 (2018) 035901. doi:10.1088/1361-6501/aa9a0b.